Synthesis, Structural, and Transport Properties of Cr-Doped BaTi$_2$As$_2$O

Qiucheng Ji,[†] Yonghui Ma,[†] Kangkang Hu,[†,‡] Bo Gao,[†] Gang Mu,[*,†] Wei Li,[†,§] Tao Hu,[†] Ganghua Zhang,[∥] Qingbiao Zhao,[∥] Hui Zhang,[∥] Fuqiang Huang,[∥] and Xiaoming Xie[†]

[†]State Key Laboratory of Functional Materials for Informatics and Shanghai Center for Superconductivity, Shanghai Institute of Microsystem and Information Technology, Chinese Academy of Sciences, Shanghai 200050, China

[‡]College of Sciences, Shanghai University, Shanghai 200444, China

[§]State Key Laboratory of Surface Physics and Department of Physics, Fudan University, Shanghai 200433, China

[∥]CAS Key Laboratory of Materials for Energy Conversion, Shanghai Institute of Ceramics, Chinese Academy of Sciences, Shanghai 200050, China

S *Supporting Information*

ABSTRACT: The interplay between unconventional super-conductivity and the ordering of charge/spin density wave is one of the most vital issues in both condensed matter physics and material science. The Ti-based compound BaTi$_2$As$_2$O, which can be seen as the parent phase of superconducting BaTi$_2$Sb$_2$O, has a layered structure with a space group $P4/mmm$, similar to that of cuprate and iron-based super-conductors. This material exhibits a charge density wave (CDW) ordering transition revealed by an anomaly at around 200 K in transport measurements. Here, we report the synthesis and systematical study of the physical properties in Cr-doped BaTi$_{2-x}$Cr$_x$As$_2$O (x = 0−0.154) and demonstrate

that the transition temperature of the CDW ordering is suppressed gradually by the doped Cr element. The magnetization measurements confirm the evolution of the CDW ordering transition. These observed behaviors are similar to that observed in iron-based superconductors, but no superconductivity emerges down to 2 K. In addition, the first-principles calculations are also carried out for well-understanding the nature of experimental observations.
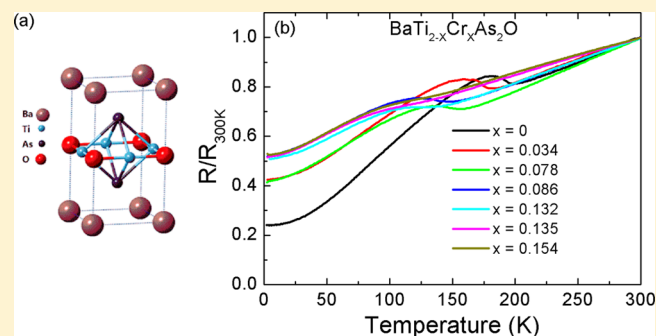
1. INTRODUCTION

Since the discovery of cuprate and iron-based superconductors,[1,2] the search for high-temperature superconductivity and novel superconducting mechanisms has become one of the most challenging tasks of condensed matter physicists and material scientists. From the viewpoint of theoretical and experimental evidence,[3−5] these superconductivities often emerge in the proximity of the ordering of spin/charge density wave instabilities, in contrast to that of conventional BCS superconductivity.[6] In recent years, the studies of the BaTi$_2$Pn$_2$O (Pn = As, Sb, Bi) system associated with charge density wave instabilities have attracted great research attentions since the discovery of the superconductor Ba$_{1-x}$Na$_x$Ti$_2$Sb$_2$O (T_c^{onset} = 5.5 K).[7] The crystal structure of BaTi$_2$Pn$_2$O combines the features of cuprate and iron-based superconductors (see Figure 1a): It consists of edge-shared [Ti$_2$Pn$_2$O] layers separated by the layers of Ba^{2+}. The conductive layer is the [Ti$_2$Pn$_2$O] layer, where the atoms show a unique connective feature. It has a Ti$_2$O square net with an anti-CuO$_2$-type structure of the cuprate superconductors, where the Pn atoms are located above and below the Ti$_2$O
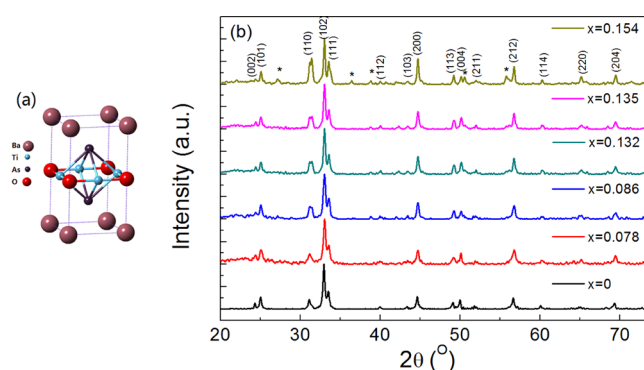

Figure 1. (a) Structure of BaTi$_2$As$_2$O. (b) X-ray diffraction patterns of BaTi$_{2-x}$Cr$_x$As$_2$O with different doping levels. Main peaks can be indexed to the layered structure of BaTi$_{2-x}$Cr$_x$As$_2$O. Small amounts of impurities are marked by the asterisks.

squares. Four Ti atoms and two Pn atoms form the octahedral sharing the corners with the neighboring one.

Interestingly, an anomalous phase transition has been observed in both the Sb- and As-based compounds by the susceptibility and resistivity measurement.[8−12] Such an anomaly was ascribed to the charge density wave order.[13] The substitution of Ba^{2+} by Na^+ in $BaTi_2Sb_2O$ as hole doping leads to the suppression of charge density wave ordering phase and the emergence of superconductivity with the highest superconducting transition temperature $T_c = 5.5$ K when $x \approx 0.15$.[7,14,15] On the other hand, Chen and co-workers successfully synthesized $BaTi_2As_2O$ in 2010 and increased the transition temperature of charge density wave order to 200 K.[16] It was reported that element doping is very difficult and only Li^+ has been doped into interstitial sites of $BaTi_2As_2O$, but no superconductivity was observed. Therefore, more efforts are needed in this system to explore the possible superconductivity and to study the nature of the interplay between super-conductivity and charge density wave (CDW) order.

In this work, chromium element was doped into $BaTi_2As_2O$, and their physical properties were fully investigated. We show the evolution of the CDW ordering transition in Ba-$Ti_{2−x}Cr_xAs_2O$ as a function of the substitution concentration. Evidences are displayed to demonstrate that, with the increase of chromium content, the CDW ordering transition temperature (T_{CDW}) is continuously lowered, but without the emergence of superconductivity down to 2 K. In addition, we carried out the first-principles calculations for both parent and doped compounds for well-understanding the nature of our experimental observations.

2. RESULTS AND DISCUSSION

The actual doping levels of the samples were analyzed and determined by the energy dispersive X-ray spectroscopy (EDS) measurements. The results can be seen in the Supporting Information, Figure S1. The values (x) determined from EDS measurements will be used in the present paper. We also examined the structure and purity of our samples by the powder X-ray diffraction (XRD) measurements at room temperature. In Figure 1b, we show the XRD data of the $BaTi_{2−x}Cr_xAs_2O$ samples with $0 \leq x \leq 0.154$. The main diffraction peaks can be indexed to the layered structure with the space group $P4/mmm$ as shown in Figure 1a. Tiny peaks from small amounts of impurities can be detected as the doping level increases. Moreover, we can see that the peaks move to the right slightly with the increase of doping, indicating the doping induced shrinkage of crystal lattice. To investigate the influences on the crystal lattice by the Cr substitution quantitatively, we obtained the lattice parameters by fitting the XRD data. The a- and c-axis lattice parameters and volume decrease gradually. The detailed descriptions and discussions about the response of crystal lattice to Cr doping are presented in the Supporting Information, Figure S2. The clear evolution of the crystal lattice suggests the successful substitution of the Cr element.

Resistance and magnetism measurements were performed to study the transport and possible superconducting properties. Figure 2 indicates the temperature dependence of normalized resistance of our samples with doping $0 \leq x \leq 0.154$. A clear anomaly is observed around 200 K for the sample with $x = 0$, which is consistent with the previous report.[16] This anomaly has been identified as a nematic CDW ordering transition.[13] For the samples in low doping region, such a transition was also detected by the magnetism measurements. Taking the sample with $x = 0.034$ as an example, the transition temperature T_{CDW}
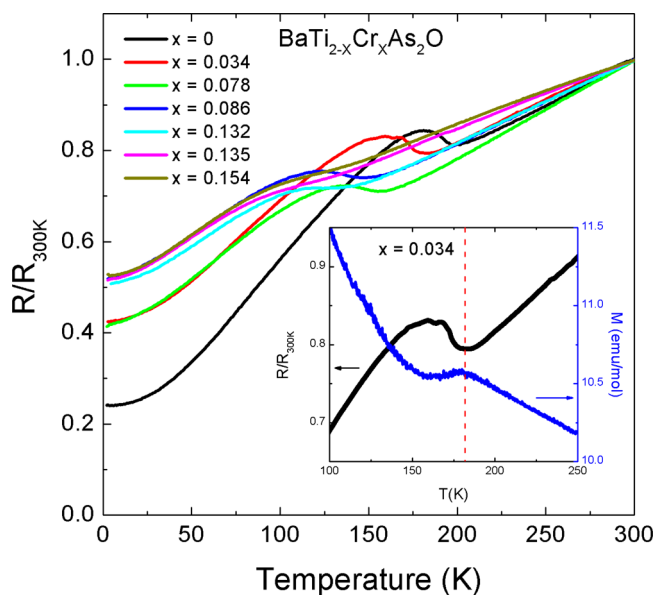

Figure 2. Temperature dependence of the resistance for Ba-$Ti_{2−x}Cr_xAs_2O$ samples, normalized to the data at 300 K. Inset is the comparison of $R−T$ and $M−T$ curves for one typical sample with $x = 0.034$ to confirm the CDW transition at T_{CDW}. The applied field of the $M−T$ curve is 1 T.

determined in the $M−T$ curve is rather consistent with that in the $R−T$ curve, as shown in the inset of Figure 2. As more and more chromium is doped into the sample, the CDW transition temperature declines gradually, but no superconductivity emerges down to 2 K.

In Figure 3, we show the doping dependence of the CDW transition temperature T_{CDW}. The dashed line is a guide for the
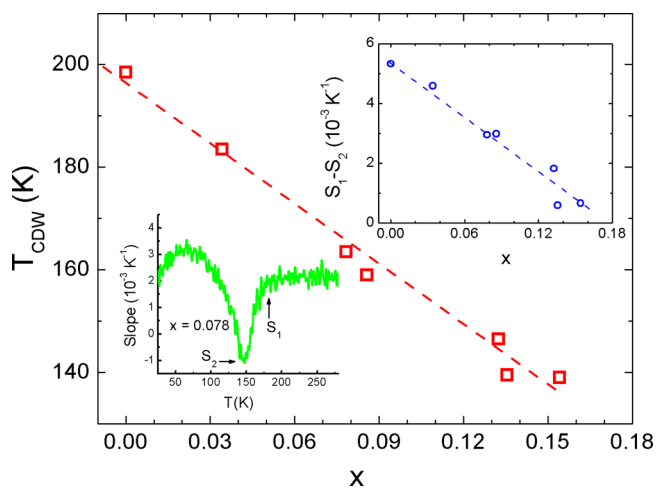

Figure 3. Doping dependence of CDW transition temperature, T_{CDW}. The dashed line is the guide for the eyes. The slope curve of the $R−T$ curve for the sample with $x = 0.078$ is plotted in the left inset. Doping dependence of $S_1 − S_2$ is shown in right inset.

eyes. T_{CDW} goes down gradually and shows a roughly linear tendency with the increase of doping concentration. The lowest T_{CDW} obtained from our experiment is 139 K. Further suppression of T_{CDW} is hampered due to the solubility limit of Cr and the indistinctive resistive features from the CDW transition in the high doping region. Here, we also attempted to describe such resistive features of the CDW transition

quantitatively. As shown in the left inset of Figure 3, the temperature derivative of resistance, slope = $d(R/R_{300K})/dT$, for the sample with $x = 0.078$ is plotted versus temperature. In this figure, the onset point of the transition S_1 and the minimum point S_2 are determined. The difference of slopes between the two points $S_1 - S_2$ is used to describe the feature due to the CDW transition. In the right inset of Figure 3, we show the doping dependence of $S_1 - S_2$. The value of $S_1 - S_2$ also decreases linearly with the doping level x and becomes nearly zero with x around 0.15, which suggests that the features due to the CDW ordering are almost unobservable in the resistance data in the high doping region.

In order to well-understand the nature of experimental observations, we carry out the first-principles calculations[17−20] to discuss the evolution of electronic structure as Cr doped in $BaTi_2As_2O$. The calculated total and projected density of states (DOS) for $BaTi_2As_2O$ and Cr doped $BaTi_{1−x}Cr_xAs_2O$ are shown in Figure 4a,b, respectively. Here, we take $x = 0.25$ to
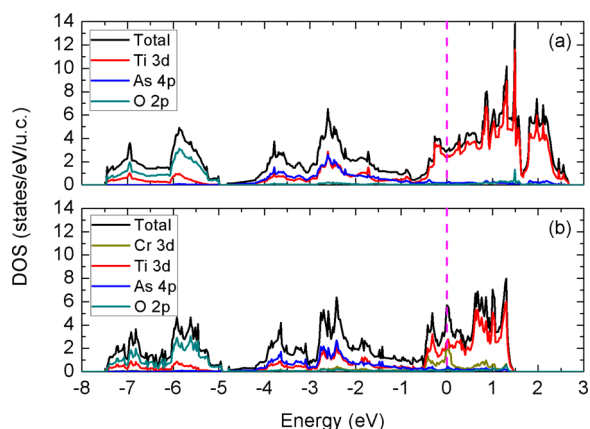

Figure 4. Total and projected DOS on Ti 3d (Cr 3d), As 4p, and O 2p orbitals per unit cell of (a) $BaTi_2As_2O$ and (b) $BaTi_{1.75}Cr_{0.25}As_2O$ in the nonmagnetic state by using GGA calculations. The Fermi energy is set to zero (dashed line).

facilitate the calculations, although it is higher than the highest doping level of our experiments. Apparently, a significant change in the total DOS can be seen by comparing the two figures, especially in the region around the Fermi level, where the bandwidth of Cr doped $BaTi_{1.75}Cr_{0.25}As_2O$ is reduced gradually in reference to that of the parent compound $BaTi_2As_2O$, resulting in the enhancement of electron correlations being consistent with our magnetism measurements (data not shown here). In addition, we notice that the doping procedure is indeed an introduction of the electron-type carriers as Cr doped into the $BaTi_2As_2O$ as expected from our intuition. The electron dopant leads to the suppression of the charge density wave order, consistent with our transport measurements.

3. CONCLUSION

In the present work, the Cr element was successfully doped into $BaTi_2As_2O$. The structure, resistance, and magnetism properties were investigated systematically. The a- and c-axis lattice parameters and volume decrease gradually. Both the transition temperature and the resistive features of the CDW ordering transition are suppressed gradually with the increase of Cr doping. No superconductivity was observed down to 2 K. The clear reduction of the bandwidth and the introduction of

electron-type carriers by the Cr doping are evidenced by the first-principles calculations.

■ ASSOCIATED CONTENT

⑤ Supporting Information

Experimental details, details of the first-principles calculations, EDS results, and lattice parameters. This material is available free of charge via the Internet at http://pubs.acs.org.

■ AUTHOR INFORMATION

Corresponding Author

*Fax: +86-21-62127493. E-mail: mugang@mail.sim.ac.cn.

Notes

The authors declare no competing financial interest.

■ ACKNOWLEDGMENTS

■ REFERENCES

(1) Bednorz, J. G.; Müller, K. A. *Z. Phys. B* **1986**, *64*, 189−193.
(2) Kamihara, Y.; Watanabe, T.; Hirano, M.; Hosono, H. *J. Am. Chem. Soc.* **2008**, *130*, 3296−3297.
(3) Lee, P. A.; Nagaosa, N.; Wen, X. G. *Rev. Mod. Phys.* **2006**, *78*, 17−85.
(4) Dong, J.; Zhang, H. J.; Xu, G.; Li, Z.; Li, G.; Hu, W. Z.; Wu, D.; Chen, G. F.; Dai, X.; Luo, J. L.; Fang, Z.; Wang, N. L. *Europhys. Lett.* **2008**, *83*, 27006.
(5) Paglione, J.; Greene, R. L. *Nat. Phys.* **2010**, *6*, 645−658.
(6) Mu, G.; Wang, Y.; Shan, L.; Wen, H. H. *Phys. Rev. B* **2007**, *76*, 064527.
(7) Doan, P.; Gooch, M.; Tang, Z. J.; Lorenz, B.; Möller, A.; Tapp, J.; Chu, C. W.; Guloy, A. M. *J. Am. Chem. Soc.* **2012**, *134* (40), 16520−16523.
(8) Ozawa, T. C.; Pantoja, R.; Axtell, E. A., III; Kauzlarich, S. M.; Greedan, J. E.; Bieringer, M.; Richardson, J. W., Jr. *J. Solid State Chem.* **2000**, *153*, 275−281.
(9) Ozawa, T. C.; Kauzlarich, S. M.; Bieringer, M.; Greedan, J. E. *Chem. Mater.* **2001**, *13*, 1804−1810.
(10) Ozawa, T. C.; Kauzlarich, S. M. *J. Cryst. Growth* **2004**, *265*, 571−576.
(11) Liu, R. H.; Tan, D.; Song, Y. A.; Li, Q. J.; Yan, Y. J.; Ying, J. J.; Xie, Y. L.; Wang, X. F.; Chen, X. H. *Phys. Rev. B* **2009**, *80*, 144516.
(12) Pickett, W. E. *Phys. Rev. B* **1998**, *58*, 4335.
(13) Frandsen, B. A.; Bozin, E. S.; Hu, H.; Zhu, Y.; Nozaki, Y.; Kageyama, H.; Uemura, Y. J.; Yin, W.-G.; Billinge, S. J. L. *arXiv.org, e-Print Arch.*, **2014**, 1405.3236.
(14) Chang, J.; Blackburn, E.; Holmes, A. T.; Christensen, N. B.; Larsen, J.; Mesot, J.; Liang, R. X.; Bonn, D. A.; Hardy, W. N.; Watenphul, A.; Von, Z. M.; Forgan, E. M.; Hayden, S. M. *Nat. Phys.* **2012**, *8*, 871−876.
(15) Lorenz, B.; Guloy, A. M.; Chu, C. W. *Int. J. Mod. Phys. B* **2014**, *28*, 1430011.
(16) Wang, X. F.; Yan, Y. J.; Ying, J. J.; Li, Q. J.; Zhang, M.; Xu, N.; Chen, X. H. *J. Phys.: Condens. Matter* **2010**, *22*, 075702.
(17) Li, W.; Setty, C.; Chen, X. H.; Hu, J. *Front. Phys.* **2014**, *9*, 465−471.
(18) Li, W.; Dong, S.; Fang, C.; Hu, J. *Phys. Rev. B* **2012**, *85*, 100407(R).

(19) Li, W.; Zhu, J.-X.; Chen, Y.; Ting, C. S. *Phys. Rev. B* **2012**, *86*, 155119.

(20) Li, W.; Li, J.; Zhu, J.-X.; Chen, Y.; Ting, C. S. *Europhys. Lett.* **2012**, *99*, 57006.

13092

dx.doi.org/10.1021/ic502192h | *Inorg. Chem.* 2014, 53, 13089−13092